JPE 3-3-6

Static VAR Compensator-Based Voltage Regulation for Variable-Speed Prime Mover Coupled Single-Phase Self-Excited Induction Generator

[1]Tarek Ahmed*, [2]Osamu Noro, [1]Shinji Sato, and [1]Mutsuo Nakaoka

[1]Division of Electrical and Electronics Systems Eng., Yamaguchi University, Yamaguchi, Japan
[2]Kawasaki Heavy Industry, Kobe, Japan

ABSTRACT

In this paper, the single-phase static VAR compensator (SVC) is applied to regulate and stabilize the generated terminal voltage of the single-phase self-excited induction generator (single-phase SEIG) driven by a variable-speed prime mover (VSPM) under the conditions of the independent inductive load variations and the prime mover speed changes. The conventional fixed gain PI controller-based feedback control scheme is employed to adjust the equivalent capacitance of the single-phase SVC composed of the fixed excitation capacitor FC in parallel with the thyristor switched capacitor TSC and the thyristor controlled reactor TCR. The feedback closed-loop terminal voltage responses in the single-phase SEIG coupled by a VSPM with different inductive passive load disturbances using the single-phase SVC with the PI controller are considered and discussed herein. A VSPM coupled the single-phase SEIG prototype setup is established. Its experimental results are illustrated as compared with its simulation ones and give good agreements with the digital simulation results for the single-phase SEIG driven by a VSPM, which is based on the SVC voltage regulation feedback control scheme.

Keywords: Single-Phase Self-Excited Induction Generator, Static VAR Compensator, Independent Power Conditioner, Small-Scale Renewable Energy Distributed Power Supply

1. Introduction

Nowadays, the wind Power generation requirements have been become increasingly more and more popular in the past few years especially after the 1970s during the energy crisis.

The use of the wind power energy for electrical generation has been started in a major way. Some applications are related to large-scale, utility-size wind parks or wind farm where thousands of various wind turbines are interconnected to generate large-scale electricity in the rural residential applications. In some other parts of the world, a variety of wind turbines are installed on a smaller scale. Most of wind turbines are equipped with line-connected induction generators. The power rating squirrel cage rotor type induction generators are more

Manuscript received May 2, 2003; revised July 30, 2003.
Corresponding Author: tarek@pe-news1.eee.yamaguchi-u.ac.jp Tel: +81-836-85-9472, Fax: +81-836-85-9401

attractive as wind turbine-coupled ac generators due to their low cost, compactness, ruggedness, high reliability, low inertia and the need for little or no maintenance. In the case of induction generator connected to a utility ac grid, its output voltage and frequency have been already determined by the utility ac power source, but in case of a stand-alone independent generating plant, the induction generator must determine and establish the output voltage and frequency by itself[1-6]. Possible and effective applications of the power conditioning and processing system for independent power supply applications are currently under investigation. The generated output voltage can be directly connected to the load facility installation and equipment are non-sensitive to the ac frequency which include an electric heater, a battery charger, a super capacitor energy storage using a diode rectifier circuit or power factor correction converter and a telecommunication energy distribution power supply which can be flexibly supplied and distributed by rectifying its output terminal voltage with the voltage regulation to provide a specified dc output voltage.

Over the past decade years, few researchers have attempted to analyze the steady-state and dynamic performance of the single-phase SEIG driven by a constant-speed prime mover[2-5].

In this paper, the authors propose a new small-scale stand-alone power generating system employing the variable-speed prime mover (VSPM) coupled the single-phase self-excited induction generator (single-phase SEIG), which is excited by the static VAR compensator (SVC). In our proposal, the absolute constant output voltage can be obtained even though the rotor shaft speed changes in accordance with the load disturbances. The closed-loop PI compensator for the terminal voltage regulation of the single-phase SEIG driven directly by a VSPM is established using the SVC, which is composed of the fixed excitation capacitor (FC) in parallel with thyristor phase controlled reactor (TCR) and thyristor switched capacitor (TSC). The operating performances in the steady-state and dynamic-state of the single-phase SEIG are evaluated and discussed as a stand-alone power conditioner on the basis of the simulation and the experimental results. The practical effectiveness of the simple rotating type power conditioner treated here is proved as rural renewable energy and power utilizations in the independent distributed load.

2. Voltage Regulation Implementation of Single-Phase SEIG Excited by PI Controlling Static VAR Compensator

The whole proposed stand-alone power conditioner voltage regulation scheme is schematically depicted in Fig. 1 for a simple wind turbine coupled a single-phase SEIG with SVC. In this system configuration, a stand-alone load is directly connected to the stator winding side of the single-phase squirrel cage rotor type SEIG and the SVC composed of FC in parallel with TCR and TSC, which is controlled by a closed-loop feedback control with a PI compensator. The stator voltage of the single-phase SEIG is controlled to be constant by the implementation of the reactive power control required for the power conditioner from the SVC under the conditions of the inductive load variations and the prime mover speed changes. The single-phase 4 poles, 220 V, 2 kW, squirrel cage rotor type induction generator supplies to a resistive load or an inductive load in stand-alone applications.

Table 1. Design Specifications and Circuit Parameters.

Items	*Machine Ratings and Machine Parameters*	
Single-Phase Squirrel Cage Rotor Induction Machine (Single-phase SEIG)	Rated Voltage	220 V
	Rated Power	2 kW
	Number of Poles	4
	Rated Frequency	50 Hz
	Rotor Type	Squirrel Cage
	Induction Machine Parameters at 50 Hz	
	R_1=1.40 ohm	X_1=2.1 ohm
	R_2=0.59 ohm	X_2=1.05 ohm
SVC composed of FC, TCR &TSC (see Fig.1)	X_{TCR} at 50 Hz;L_{TCR}	56 ohm, 0.18 H
	X_C at 50 Hz; C	13 ohm, 244 μF
	X_{TSC} at 50 Hz; C_{TSC}	32 ohm, 100 μF
PI Controller	K_P	See Fig.3
	K_I	See Fig.3
VSPM (Modeling by dc Motor)	τ_o(see eqn.(1))	See Fig.4
	υ_o(see eqn.(1))	See Fig.4
Inductive Load Components	R_L	35-200 ohm
	X_L at 50 Hz	25-140 ohm

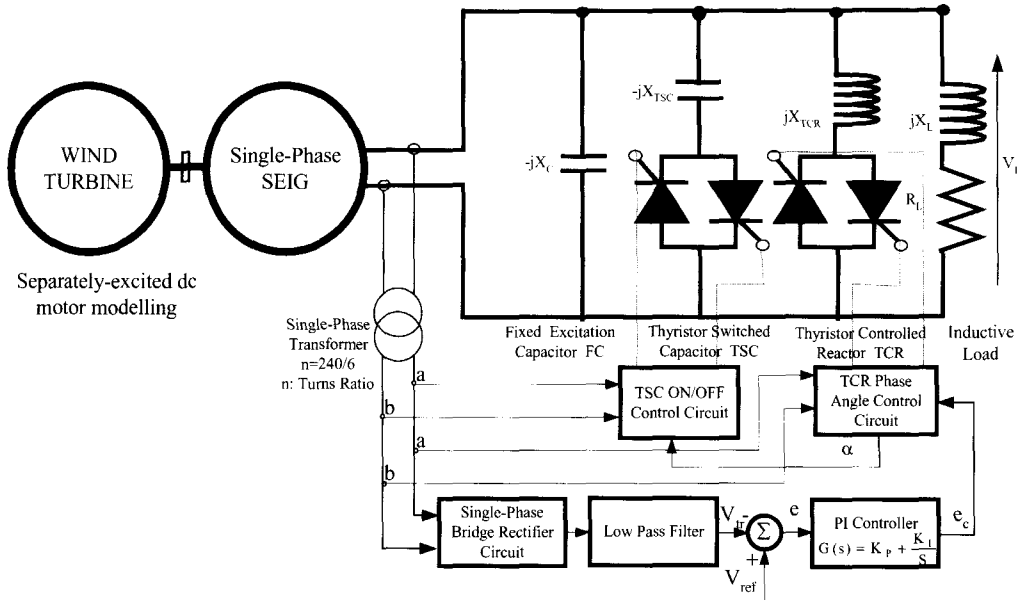

Fig. 1. Schematic system configuration of single-phase SEIG excited by SVC for its voltage regulation.

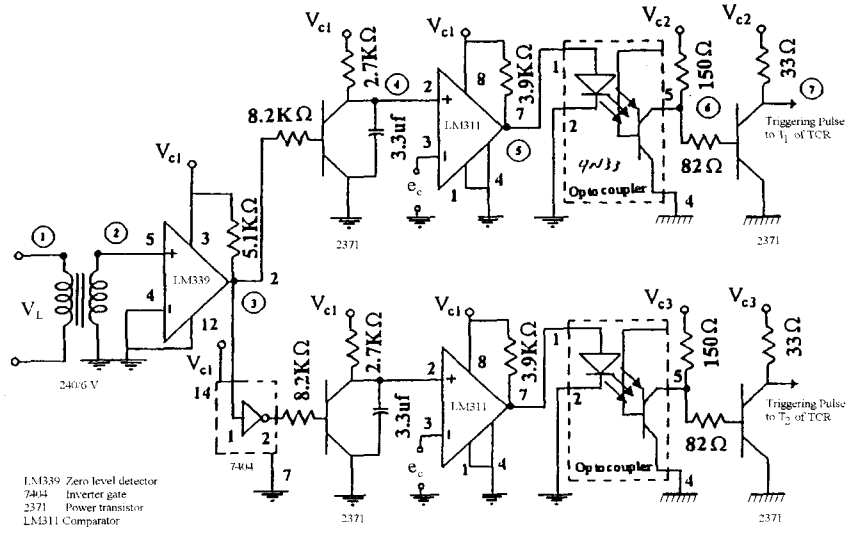

Fig. 2. Designed thyristors triggering circuit for TCR.

The thyristor triggering pulse control circuit for the TCR and the PI controller circuit in a feedback control scheme are designed and shown in Fig. 2 and Fig. 3, respectively, for the purpose of regulating the single-phase SEIG generated terminal voltage. Table 1 includes the design specifications and circuit parameters of the voltage regulation system description for the single-phase SEIG with the SVC adjusted by the PI controller in the feedback control loop implementation.

3. Torque-Speed Characteristics of Variable-Speed Prime Mover

The mechanical output power P_m of the VSPM is defined as[1],

$$P_m = (\tau_o - \upsilon_o \upsilon)\omega_s \upsilon \quad (1)$$

where, υ is the per unit speed of the VSPM ($\upsilon = N/N_s$), N

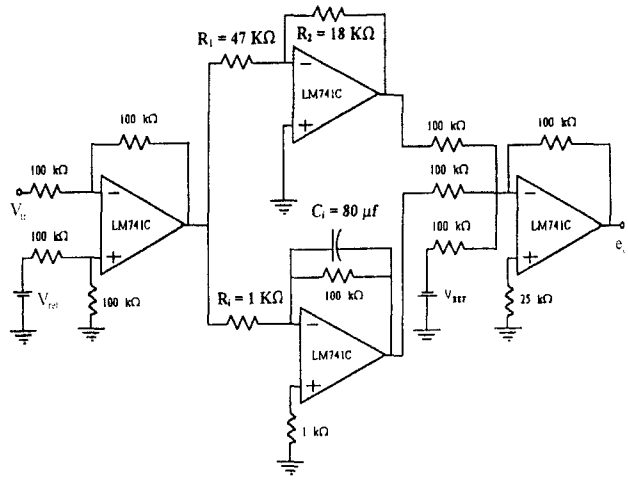

Fig. 3. Designed PI controller circuit.

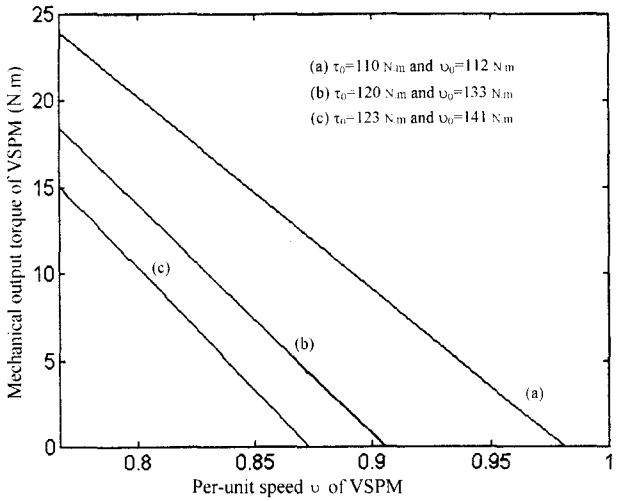

Fig. 4. Mechanical output torque characteristics of VSPM against its per-unit shaft speed.

and N_s are the rotor speed and the single-phase SEIG synchronous speed in (rpm), respectively. ω_s is the rated synchronous angular speed ($\omega_s = 2\pi N_s/60$). τ_o and υ_o respectively are the torque coefficient and speed coefficient in N.m. In experiment, a controllable separately excited dc motor is used with a constant armature voltage and a field current control. Fig. 4 illustrates the effect of the field current control on the torque speed characteristics and the corresponding torque-speed coefficients τ_o and υ_o which are given by,

$$\tau_o = \frac{K_t \phi_m V_a}{R_a} \quad \text{and} \quad \upsilon_o = \frac{2\pi K_t^2 \phi_m^2}{60 R_a} N_s$$

where, K_t is the torque constant, ϕ_m is the field flux in Wb per pole of the dc motor, V_a is the armature voltage in volt and R_a is the armature resistance in ohm.

4. Static VAR Compensator for Voltage Regulation of Single-Phase SEIG

Capacitors are routinely placed in parallel with inductive loads connected to the constant voltage and frequency utility ac grid for power factor improvement. If the inductive load connected to the utility ac power source has a constant reactive volt-ampere (VAR) requirement, a fixed capacitor can be selected to correct the power factor to be unified. However, if this inductive load has a varying VAR requirement, the fixed-capacitor arrangement results in a changing power factor. The circuit of Fig. 1 represents an application of an ac voltage controller to maintain a constant generated terminal voltage of the single-phase SEIG with varying the load VAR requirements. The voltage regulation fixed excitation capacitance supplies a fixed amount of reactive power, generally more than the required for both the inductive load and the single-phase SEIG. The parallel inductance of the TCR absorbs a variable amount of the reactive power, depending on the delay angle of the SCRs. The net reactive power supplied by the inductor-capacitor combination is controlled to match that absorbed by the load and the single-phase SEIG to keep its generated terminal voltage is constant. As the VAR requirement of the load changes, the delay angle is adjusted to maintain a constant generated terminal voltage of the single-phase SEIG. This type of terminal voltage regulation is known as a static VAR control. (The SCRs are placed in the inductor branch rather than in the capacitor branch because very high currents could results from switching a capacitor with an SCR.). Static VAR control has the advantage of being able to adjust to changing load requirement very quickly. Reactive power is continuously adjustable with static VAR control, rather than having discrete levels, as with capacitor banks, which are switched in and out with circuit breakers or anti-parallel on/off control thyristors; TSC. Static VAR control is becoming increasingly prevalent in installations with rapidly varying reactive power requirements, such as electric arc furnaces.

The instantaneous reactor current flowing through the inductor of TCR shown in Fig. 1 with the thyristor triggering delay angle α is expressed by[7],

$$i_{TCR}(t)=\begin{cases}\dfrac{\sqrt{2}V_L}{X_{TCR}}(\cos\alpha-\cos\omega t) & \alpha\le\omega t\le\alpha+\sigma\\ 0 & \sigma+\alpha\le\omega t\le\alpha+\pi\end{cases} \quad (2)$$

where, α is the thyristor triggering delay angle with respect to the zero crossing output voltage waveform, σ is the conduction angle of the thyristor, X_{TCR} is the equivalent inductive reactance of TCR inductor. V_L is the effective value of the single-phase SEIG generated output voltage and ω is the electrical angular frequency. With neglecting the harmonic currents generated by the switched inductances, the fundamental component of the TCR inductive reactor current defined previously as the above equation is obtained on the basis of using the Fourier series expansion as follows,

$$I_{TRCI}=B_{TCR}(\sigma)V_L \quad (3)$$

where B_{TCR} is the equivalent inductive susceptance of the TCR and defined a function of the conduction angle σ as,

$$B_{TCR}(\sigma)=\frac{\sigma-\sin\sigma}{\pi X_{TCR}} \quad (4)$$

$$\text{where } \alpha+\frac{\sigma}{2}=\pi \quad (5)$$

The control range of the thyristor triggering delay angle α is between $\pi/2$ and π. Observing (4), the control range of the conduction angle σ corresponding to the control range of α will be between π and zero.

5. Steady-State Analysis and Operating Performances of single-Phase SEIG Excited by Static VAR Compensator

The single-phase SEIG electro-mechanical equivalent circuit excited by the SVC is depicted in Fig. 5. The equivalent inductive susceptance B_{TCR} of the TCR, which is a function of the thyristor conduction angle σ and the capacitive reactance X_{TSC} of the TSC which is switched on under the conditions of the terminal voltage of the single-phase SEIG is less than the desired or reference voltage; 220 and the conduction angle σ=0 of the TCR or the triggering delay angle $\alpha=\pi$ are connected in parallel with the fixed excitation reactance X_C terminal ports as shown in Fig. 5[4][5].

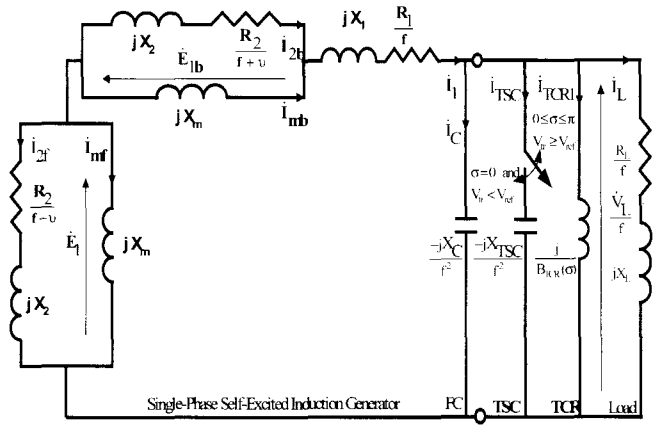

Fig. 5. Approximate electro-mechanical equivalent circuit of single-phase SEIG with SVC.

In Fig. 5, f is the per-unit frequency, (f=F/F_b, F and F_b are the generated output frequency and base frequency of the single-phase SEIG; F_b=50Hz), R_1, X_1, R_2 and X_2 are the single-phase induction generator parameters referred to the stator winding side, R_L and X_L are the inductive load components in ohm, X_C ($X_C=1/2\pi F_b C$; F_b=50Hz and C is the fixed excitation capacitance in farad) is the fixed excitation reactance in ohm, X_{TSC} is the capacitive reactance of the TSC, X_m is the magnetizing reactance in ohm, $\dot{E}_1$, $\dot{E}_{1b}$, $\dot{V}_L$, $\dot{I}_1$, $\dot{I}_{2f}$, $\dot{I}_{2b}$, $\dot{I}_{mf}$, $\dot{I}_{mb}$, $\dot{I}_L$, $\dot{I}_C$ and $\dot{I}_{TSC}$ are the air gap voltage due to the forward rotating field in volt, the air gap voltage due to the backward rotating field in volt, the single-phase SEIG generated terminal voltage in volt, the stator current in ampere, the forward rotating field rotor current referred to the stator side in ampere, the backward rotating field rotor current referred to the stator side in ampere, the magnetizing current of the forward rotating field, the backward rotating field magnetizing current, the inductive load current in ampere, the fixed excitation capacitive current of FC in ampere and the capacitive reactance current of the TSC in ampere for the single-phase SEIG, respectively.

5.1 Per-unit frequency and Per-unit Speed of single-phase SEIG

The steady-state circuit analysis of the single-phase SEIG controlled by the SVC connected to its terminal ports is derived as follows. By observing the approximate electro-mechanical equivalent circuit of the single-phase SEIG illustrated in Fig. 5, the squirrel cage rotor current I_{2f} referred to the stator winding side of the single-phase SEIG excited by the SVC can be expressed by,

$$I_{2f} = \frac{E_1}{R_2\sqrt{\frac{1}{(f-\upsilon)^2}+\left(\frac{X_2}{R_2}\right)^2}} \tag{6}$$

The term (f-υ) is usually extremely small from a practical point of view. As a result, the term (X_2^2/R_2^2) could be substantially neglected with respect to $[1/(f-\upsilon)^2]$. Eq. 6 of the rotor current I_{2f} referred to the stator circuit side can be expressed by the following equation,

$$I_{2f} = \frac{(f-\upsilon)E_1}{R_2} \tag{7}$$

The mechanical input power P_i of the single-phase induction machine can be written as the references[1],

$$P_i = -I_{2f}^2 \frac{R_2}{(f-\upsilon)}\left(\frac{\upsilon}{f}\right) \tag{8}$$

By substituting I_2 in (7) into (8) and making the mechanical power balance from the principle of the energy conversion through equating (8) to (1). The per unit speed υ can be obtained as follows:

$$\upsilon = \frac{(\tau_0 + \frac{E_1^2}{R_2\omega_s})f}{\upsilon_0 f + \frac{E_1^2}{R_2\omega_s}} \tag{9}$$

5.2 Series impedance approach for steady-state circuit analysis of single-phase SEIG

By applying the series impedance approach on the per-phase approximate equivalent circuit of the single-phase SEIG with SVC depicted in Fig. 5, the following equation can be written as follows,

$$(\dot{Z}_{sr} + \dot{Z}_{rm} + \dot{Z}_{ms})\dot{I}_1 = 0 \tag{10}$$

But $\dot{I}_1$ does not equal to zero for the generated terminal voltage of the single-phase SEIG, the following series impedance relationship yields,

$$(\dot{Z}_{sr} + \dot{Z}_{rm} + \dot{Z}_{ms}) = 0 \tag{11}$$

With neglecting the magnetizing reactance X_m in the negative-sequence rotor branch of the single-phase SEIG depicted in Fig.5 as compared with the negative-sequence rotor branch $[R_2/(f+\upsilon)+jX_2]$, $\dot{Z}_{sr}$, $\dot{Z}_{rm}$ and $\dot{Z}_{ms}$ can be represented as,

$$\dot{Z}_{sr} = \frac{(\frac{R_L}{f} + jX_L)(-j\frac{X_C + X_{TSC}}{f^2 - B_{TCR}(X_C + X_{TSC})})}{\frac{R_L}{f} + j(X_L - \frac{X_C + X_{TSC}}{f^2 - B_{TCR}(X_C + X_{TSC})})} \tag{12}$$

$$\dot{Z}_{rm} = \frac{\left(\frac{R_2}{f-\upsilon} + jX_2\right)(jX_m)}{\left[\frac{R_2}{f-\upsilon} + j(X_2 + X_m)\right]} \tag{13}$$

$$\text{and } \dot{Z}_{ms} = \frac{R_1}{f} + \frac{R_2}{f+\upsilon} + j(X_1 + X_2) \tag{14}$$

The two non-linear simultaneous equations of the magnetizing reactance X_m as a function of the per-unit frequency f with susceptance B_{TCR} (see (4)) to be controlled by the PI controller and connected in parallel with X_C and X_{TSC} are obtained by equating the imaginary and real parts of (11) to zero and arranged as follows,

$$X_m = -\frac{C_0 + C_1 f + C_2 f^2 + C_3 f^3 + C_4 f^4 + C_5 f^5 + C_6 f^6}{(A_0 + A_1 f + A_2 f^2 + A_3 f^3 + A_4 f^4) f^2} \tag{15}$$

$$X_m = \frac{D_0 + D_1 f + D_2 f^2 + D_3 f^3 + D_4 f^4 + D_5 f^5 + D_6 f^6}{B_0 + B_1 f + B_2 f^2 + B_3 f^3 + B_4 f^4 + B_5 f^5 + B_6 f^6} \tag{16}$$

Through equating and crossing multiplication (15) and (16), the 12th degree polynomial equation represented in the per unit frequency f is derived by,

$$Y_{12} f^{12} + Y_{11} f^{11} + Y_{10} f^{10} + Y_9 f^9 + Y_8 f^8 + Y_7 f^7 + Y_6 f^6 + Y_5 f^5 + Y_4 f^4 + Y_3 f^3 + Y_2 f^2 + Y_1 f + Y_0 = 0 \tag{17}$$

where, the real coefficients from Y_0 to Y_{12} can be systematically expressed in terms of constants A_i (i=0~4), B_j (j=0~6) , C_k (k=0~6) and D_l (l=0~6) which are indicated in Appendix.

5.3 Output Voltage Characteristic of Single-Phase SEIG

The per-unit frequency f can be determined from (17) by using Newton Raphson method and then substitute the per-unit frequency f into the (15) or (16) to calculate the magnetizing reactance X_m. The air gap voltage E_1 is evaluated from the magnetization characteristic, which is the relationship between the air gap voltage E_1 and the magnetizing reactance X_m of the forward rotating field. To determine the magnetization curve of the single-phase SEIG, the single-phase induction machine is driven at the rated synchronous speed Ns=1500 rpm and a single-phase variable voltage ac supply is supplied to its stator winding at the rated frequency 50Hz[1-5]. According to the above conditions, the slip; s of the single-phase induction motor is equal to zero and hence the positive-sequence rotor branch is equivalently opened. Also, the magnetizing reactance in the negative-sequence rotor branch of the single-phase induction motor could be neglected as compared with the negative-sequence rotor branch. Therefore, the magnetizing reactance X_m is estimated using the equivalent circuit shown in Fig. 5 without FC, TSC, TCR and the load impedance by,

$$X_m = \sqrt{(\frac{V_s}{I_S})^2 - (R_1 + \frac{R_2}{2})^2} - (X_1 + X_2) \tag{18}$$

where the experimental data of the single-phase supply voltage V_s against the supply current I_s is indicated in Fig. 6. The air gap voltage E_1 is calculated by,

$$E_1 = I_s X_m \tag{19}$$

The relation between the air gap voltage E_1 and the magnetizing reactance X_m is obtained experimentally and depicted in Fig. 7. To evaluate the single-phase SEIG output voltage characteristics, the magnetization curve obtained experimentally is represented with a piece-wise linear characteristics by the following equation giving a sufficiently good mapping of the air gap voltage E_1 versus the magnetizing reactance X_m nonlinear curve and given by,

$$E_1 = \begin{cases} 342.86 - 5.850X_m & X_m \le 22.69 \\ 450.00 - 3.773X_m & 22.69 \le X_m \le 25.77 \\ 871.43 - 26.860X_m & 25.77 \le X_m \le 27.12 \\ 0 & X_m \ge 27.12 \end{cases} \tag{20}$$

Observing Fig. 5, the terminal voltage of the single-phase SEIG can be defined as,

$$V_t = fE_1 \frac{|\dot{Z}_{sr}|}{|\dot{Z}_{sr} + \dot{Z}_{ms}|} \tag{21}$$

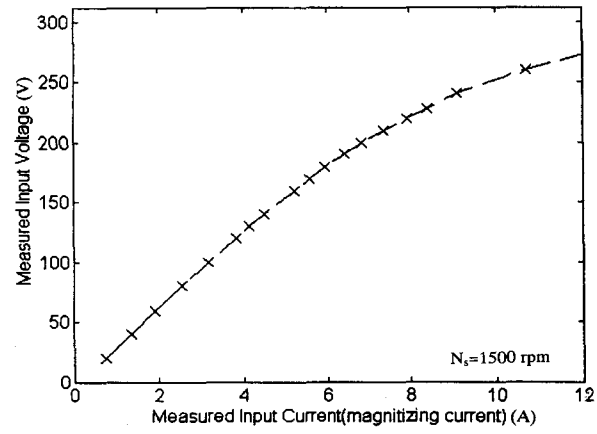

Fig. 6. Supply voltage against supply current of single- phase induction motor at no load.

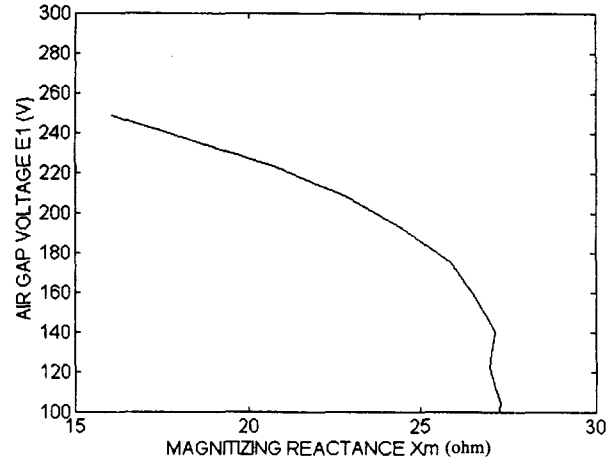

Fig. 7. Air gap voltage vs. magnetizing reactance of single-phase induction machine.

6. PI controller for Voltage Regulation of Single-Phase SEIG

The Laplace transformation of the output signal $E_c(s)$ of the PI controller shown in Fig.1 is indicated by,

$$E_c(s) = \left(K_P + \frac{K_I}{s} \right) (V_{ref}(s) - V_{tr}(s)) \quad (22)$$

where, $V_{ref}(s)$, $V_{tr}(s)$ are the Laplace transformation of the reference voltage and rectified voltage proportional to the output voltage of the single-phase SEIG, respectively, K_P and K_I are the Proportional gain and Integral gain of the PI controller, respectively. The above equation can be expressed in the discrete form as follow,

$$E_c(k) = E_c(k-1) + (K_p + T_s K_I)\left[V_{ref}(k) - V_{tr}(k)\right] - K_P\left[V_{ref}(k-1) - V_{tr}(k-1)\right] \quad (23)$$

where, $[V_{ref}(k)-V_{tr}(k)]$ is the terminal voltage error at the sampling time k, $[V_{ref}(k-1)-V_{tr}(k-1)]$ is the error signal at the sampling time (k-1), T_s is the sampling period(sec).

7. Performance Results and Discussions

7.1 Reference voltage disturbances

The PI controlled feedback closed-loop voltage regulation scheme of the single-phase SEIG driven by the VSPM is designed on the basis of the static VAR compensator (SVC) and expressed in Fig. 1. The reference voltage disturbances are applied to test and verify the closed-loop terminal voltage regulation of the single-phase SEIG coupled by a VSPM and supplied an inductive passive load using the single-phase SVC with the PI controller. For an inductive load with 0.8 lagging power factor (R_L=90 ohm and X_L=68 ohm) and a fixed excitation capacitance (C=244μF) in parallel with the TCR (X_{TCR}=56 ohm), the digital simulation results and experimental ones of the generated terminal voltage response of the single-phase SEIG driven by a VSPM with a certain torque-speed characteristic (τ_0=120, υ_0=133, as shown in Fig. 4) and excited by SVC with the reference voltage disturbances which is defined as the actual desired output terminal voltage of the single-phase SEIG are depicted in

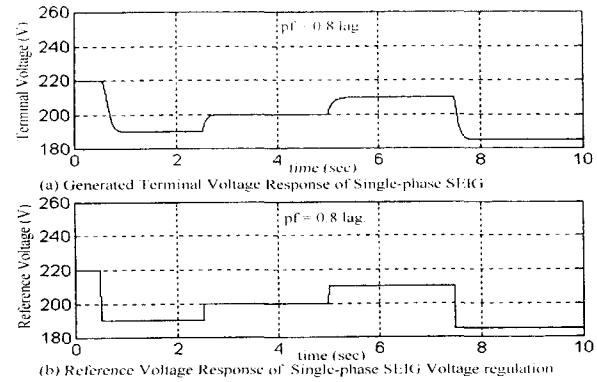

Fig. 8. Single-phase SEIG terminal voltage and reference voltage responses in case of using SVC composed of FC and TCR with 0.8 lagging power factor load.

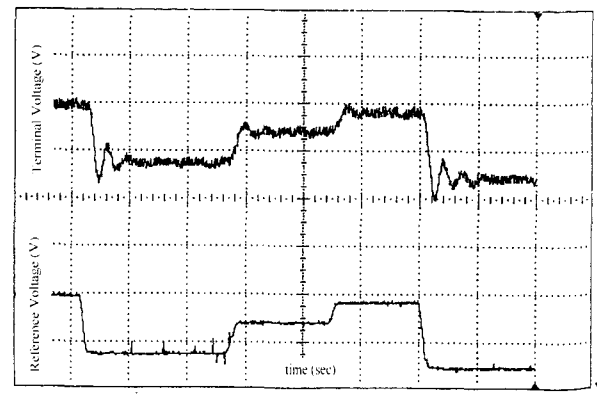

Fig. 9. Single-phase SEIG experimental terminal voltage and reference voltage responses in case of using SVC composed of FC and TCR with 0.8 lagging power factor load.

Fig. 8 and Fig. 9, respectively. The simple PI control-based SVC for the voltage regulation of the single-phase SEIG driven by the VSPM proves its feasible utilization and ability for stabilizing and regulating the single-phase SEIG terminal voltage.

7.2 Steady-State Simulation Results for Single-Phase SEIG Voltage Regulation

The steady-state analysis of the VSPM coupled single-phase SEIG excited by the SVC for its voltage regulation as a stand-alone system is based on its equivalent circuit depicted in Fig. 5 and derived as explained in section 5. The inductive load, as stand-alone equipment, is changed for observing and testing the action of the SVC to regulate and stabilize the terminal voltage

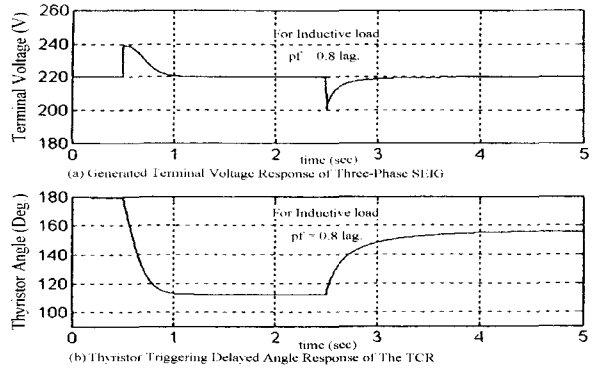

Fig. 10. Single-phase SEIG terminal voltage and TCR thyristor triggering angle responses in case of using SVC composed of FC and TCR under the condition of load variations with 0.8 lagging power factor.

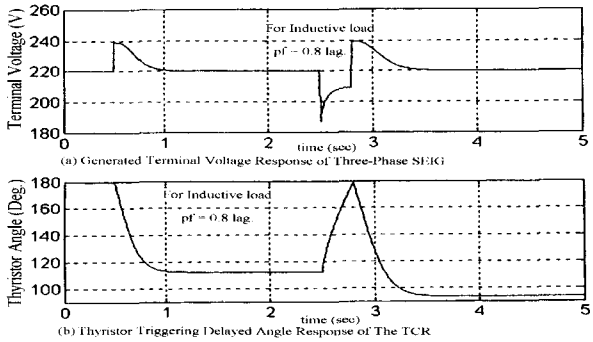

Fig. 11. Single-phase SEIG terminal voltage and TCR thyristor triggering angle responses in case of using SVC composed of FC, TSC and TCR under the condition of load variations with 0.8 lagging power factor.

of the single-phase SEIG driven by the VSPM with a certain torque-speed characteristic (τ_0=120, υ_0=133). Fig. 10(a) illustrates the terminal voltage response of the single-phase SEIG driven by the VSPM due to the inductive load variations and at the same time the prime mover speed variations according to the torque-speed characteristic shown in Fig. 4. While Fig. 10(b) shows the thyristor triggering delay angle response of the TCR. The SVC composed of TCR and FC can regulate the generated terminal voltage under the condition of a certain reactive power required by the single-phase SEIG and the inductive load. To increase the output power of the single-phase SEIG, the maximum excitation capacitance of the SVC composed of FC and TCR equals to the fixed excitation capacitance FC when the TCR is off state. At this condition, the capacitance of FC is not sufficient to increase the terminal voltage of the single-phase SEIG above the reference voltage. To increase the operating allowable range of the output power of the single-phase SEIG with its terminal voltage regulation, an additional capacitance is required to increase the terminal voltage of the single-phase SEIG above the reference voltage. The thyristor switched capacitor; TSC is connected in parallel with the TCR and the FC as shown in Fig. 11.

7.3 Experimental Results for Single-Phase SEIG Voltage Regulation

Fig. 1 illustrates the terminal output voltage regulation feedback closed-loop system including the single-phase SEIG block diagram with SVC and driven by a VSPM with a certain torque-speed characteristic (τ_0=120, υ_0=133). To validate and test the practical effectiveness of the SVC for regulating and stabilizing the terminal voltage of the single-phase SEIG driven by a VSPM, an inductive load with 0.8 lagging power factor are connected on the single-phase SEIG terminal ports. The measured single-phase SEIG voltage regulation response and the TCR trigging angle response due to the inductive passive load variations under the conditions of increasing the load impedance value using the SVC composed of FC in parallel with TCR and then decreasing the load impedance value until the terminal voltage is decreased than the reference value; 220 V using TCR in parallel with FC and TSC switched on manually are represented in Fig. 12, Fig. 13, respectively.

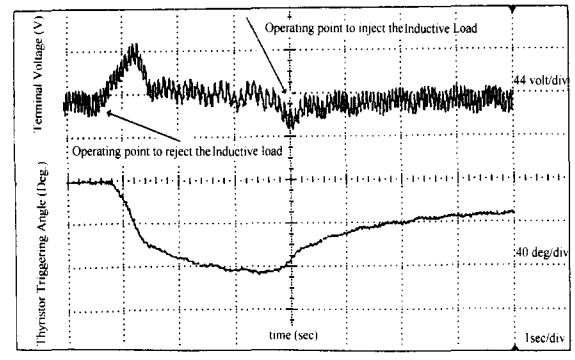

Fig. 12. Single-phase SEIG experimental terminal voltage and thyristor triggering angle responses in case of using SVC composed of FC and TCR under load variations with 0.8 lagging power factor.

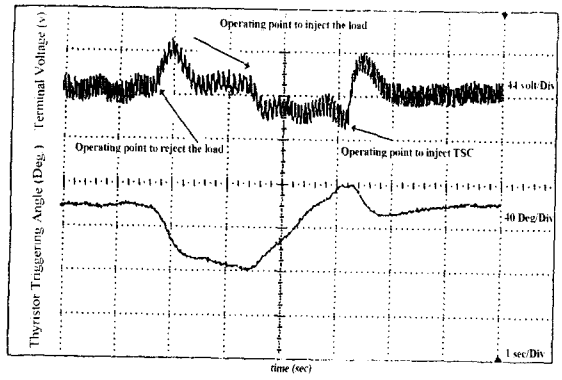

Fig. 13. Single-phase SEIG experimental terminal voltage and thyristor triggering angle responses in case of using SVC composed of FC, TSC under TCR under load variations with 0.8 lagging power factor.

8. Conclusions

The present paper has introduced the PI controller-based feedback control scheme using the single-phase SVC composed of the FC in parallel with the TCR and the TSC implemented for the stable generated terminal voltage regulation of the single-phase SEIG driven by a variable-speed prime mover VSPM and loaded by different independent inductive loading conditions. The VSPM coupled single-phase SEIG exited by the SVC prototype setup has established for simple structure, low cost, downsizing in physical volumetric size, ruggedness, low inertia rotor, maintenance free, high reliability and simple control strategy in stable wind turbine driven power conditioner in the rural alternative energy effective utilization area from an earth environmental protection point of view. The feasible experimental results have good agreements with those obtained from the digital simulation ones.

Appendix

A0=G0W0+G2(T0-X2Z0)
A1=G0W1+G1W0+G2(T1-X2Z1)+G3(T0-X2Z0)
A2=G0W2+G1W1+G2(T2-X2Z2)+G3(T1-X2Z1)
A3=G0W3+G1W2+G2(T3-X2Z3)+G3(T2-X2Z2)
A4=G1W3+G3(T3-X2Z3)

D0=G0T0-G2F0X2,
D1=G0T1+G1T0-G2F1X2-G3F0X2,
D2=G0T2+G1T1-G2F2X2-G3F1X2,
D3=G0T3+G1T2-G2F3X2-G3F2X2,
D4=G1T3-G2F4X2-G3F3X2,
D5=-G2F5X2-G3F4X2,
D6=-G3F5X2,

C0=G0F0,
C1=G0F1+G1F0,
C2=G0F2+G1F1+G2T0X2,
C3=G0F3+G1F2+G2T1X2+G3T0X2,
C4=G0F4+G1F3+G2T2X2+G3T1X2,
C5=G0F5+G1F4+G2T3X2+G3T2X2,
C6=G1F5+G3T3X2,

B0=G0Z0+G2F0,
B1=G0Z1+G1Z0+G2F1+G3F0,
B2=G0Z2+G1Z1+G2(F2+X2W0)+G3F1,
B3=G0Z3+G1Z2+G2(F3+X2W1)+G3(F2+X2W0),
B4=G1Z3+G2(F4+X2W2)+G3(F3+X2W1),
B5=G2(F5+X2W3)+G3(F4+X2W2),
B6=G3(F5+X2W3),

Y0=B0C0
Y1=B0C1+B1C0
Y2=A0D0+B0C2+B1C1+B2C0
Y3=A0D1+A1D0+B0C3+B1C2+B2C1+B3C0
Y4=A0D2+A1D1+A2D0+B0C4+B1C3+B2C2+B3C1 +B4C0
Y5=A0D3+A1D2+A2D1+A3D0+B0C5+B1C4+B2C3 +B3C2+B4C1+B5C0
Y6=A0D4+A1D3+A2D2+A3D1+A4D0+B0C6+B1C5 +B2C4+B3C3+B4C2+B5C1+B6C0
Y7=A0D5+A1D4+A2D3+A3D2+A4D1+A5D0+B1C6 +B2C5+B3C4+B4C3+B5C2+B6C1
Y8=A0D6+A1D5+A2D4+A3D3+A4D2+B2C6+B3C5 +B4C4+B5C3+B6C2
Y9=A1D6+A2D5+A3D4+A4D3+B3C6+B4C5+B5C4 +B6C3
Y10=A2D6+A3D5+A4D4+B4C6+B5C5+B6C4
Y11=A3D6+A4D5+B5C6+B6C5
Y12=A4D6+B6C6

where G0=E12/ωs, G1= υ0R2, G2=-τ0, G3=υ0,

G4=E12/ωs+R1[2E12/(ωsR2)+τ0],
G5=υ0(R2+R1), G6=2E12/(ωsR2)+τ0,
XCE=XC+XTSC

T0=XCEG4(XLBTCR+1)
+XCEG6[(X1+X2)RLBTCR+RL],
T1=XCEG5(XLBTCR+1)
+XCEG3[(X1+X2)RLBTCR+RL],
T2=-XLG4-RLG6(X1+X2),
T3=-XLG5-RLG3(X1+X2),

F0=-XCE(RLBTCR)G4,
F1=-XCE(RLBTCR)G5,
F2=RLG4+XCEG6[(X1+X2)XLBTCR+XL+X1+X2],
F3=RLG5+XCEG3[(X1+X2)XLBTCR+XL+X1+X2],
F4=-G6(X1+X2)XL,
F5=-G3(X1+X2)XL,

W0=XCE(XLBTCR+1)G6,
W1=XCE(XLBTCR+1)G3,
W2=-XLG6,
W3=-XLG3,

Z0=-XCE(RLBTCR)G6,
Z1=-XCE(RLBTCR)G3,
Z2=RLG6,
Z3=RLG3,

References

[1] S. Rajakarvna and R. Bonert, "A Technique for The Steady state Analysis of Self-Excited Induction Generator with variable speed", IEEE Trans. on Energy Conversion, Vol. 10, No. 1 pp. 10-16, March 1995.

[2] T.F. Chan, "Analysis of A Single-Phase Self-Excited Induction Generator", Electric Machine and Power Systems, Vol. 23, pp.149-162, 1995.

[3] O. Ojo and I. Bhat, "An Analysis of Single-Phase Self-Excited Induction Generators: Model Development and Steady-State Calculations", IEEE Trans. on Energy Conversion, Vol. 10, No. 2 pp. 254-260, June 1995.

[4] T. Ahmed, O. Noro, K. Sato, E. Hiraki, and M. Nakaoka, "Single-Phase Self-Excited Induction Generator with Static VAR Compensator Voltage Regulation for Simple and Low Cost Stand-Alone Renewable Energy Utilizations Part I: Analytical Study", KIEE International Trans. on Power Eng., Vol. 3-A, No. 1, pp. 17-26, 2003.

[5] T. Ahmed, O. Noro, K. Sato, E. Hiraki, and M. Nakaoka, "Single-Phase Self-Excited Induction Generator with Static VAR Compensator Voltage Regulation for Simple and Low Cost Stand-Alone Renewable Energy Utilizations Part II: Simulation and Experimental Results", KIEE International Trans. on Power Eng., Vol. 3-A, No. 1, pp. 27-34, 2003.

[6] R. Leidhold, G. Garcia, and M.I. Valla, "Induction generator Controller Based on the Instantaneous Reactive Power Theory", IEEE Trans. on Energy Conversion, Vol. 17, No. 3 pp. 368-373, Sept. 2002.

[7] IEEE Special Stability Controls Working Group Report, "Static VAR Compensator Models for Power Flow and Dynamic Performance Simulation", IEEE Trans. on Power Systems, Vol. 9, No. 1 Feb. 1994.

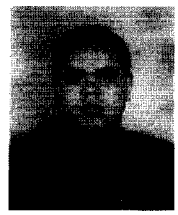

Tarek Ahmed received his M Sc.-Eng from the Electrical Engineering Department, Assiut Univ., Egypt in 1998. He is currently a Ph. D. candidate student in the Graduate School of Science and Engineering, the Power Electronic System and Control Eng. Lab. at Yamaguchi Univ., Yamaguchi, Japan. His research interests are in the area of the new applications for the power electronic circuits and systems with the renewable energy and power systems and semiconductor power conditioners.

Mr. Ahmed is a student-member of the IEEE and the Japan Society of the Power Electronics.

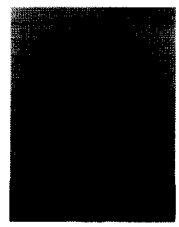

Osamu Noro received his M. Sc. in Applied Mathematics and Physics from Kyoto Univ., Kyoto, Japan. He is currently the manager of the Power Electronic Section, Development Dept.-1, System Technology Development Center of Kawasaki Heavy Industries Ltd., Akashi, Japan. His research interests are in the applications of systems technology consisting of the power electronics and electric machines such as turbine generator system, motor drive, electric and mechanical power conversion systems and so on. He is a member of IEEE and the Japan Society of Mechanical Engineers.

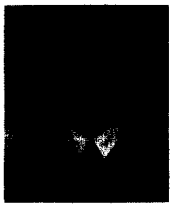

Shinji Sato graduated from Mechanical Engineering, Technical Collage of Nigata East High School. He joined in the research project at Toshiba Corporation, Tokyo. After that, he joined in research and development of Sanken Electric, Co. Ltd. Saitama. He is now studying in the Power Electronic System Laboratory, the Graduate School of Science and Engineering, Yamaguchi University, Yamaguchi, Japan. His research area includes the soft-switching PWM rectifiers and DC-DC converters. He received the 2002 paper award in IEE-IAS-Japan. He is a member of Japan Society of System, Information and Control Engineers and Japan Society of Power Electronics.

Mutsuo Nakaoka received his Dr-Eng. degree in Electrical Engineering from Osaka University, Osaka, Japan in 1981. He joined the Electrical and Electronics Engineering Department of Kobe University, Kobe, Japan in 1981. Since 1995, he has been a professor of the Electrical and Electronics Engineering Department, the Graduate School of Science and Engineering, Yamaguchi University, Yamaguchi, Japan. His research interests include application developments of power electronics circuit and systems. He received the 2001 premium paper award from IEE-UK and so on. Dr. Nakaoka is a member of the Institute of Electronics, Information and Communication Engineers of Japan, Institute of Illumination Engineering of Japan, European Power Electronics Association, the Japan Society of the Solar Energy, IEE-Korea and IEEE.